Applied Catalysis A: General 467 (2013) 7–16

Contents lists available at SciVerse ScienceDirect

Applied Catalysis A: General

journal homepage: www.elsevier.com/locate/apcata

Synthesis, characterization and catalytic properties of magnetic nanoparticle supported guanidine in base catalyzed synthesis of α-hydroxyphosphonates and α-acetoxyphosphonates

Amin Rostami[a,b,*], Bahareh Atashkar[a], Darush Moradi[a]

[a] Department of Chemistry, Faculty of Science, University of Kurdistan, Zip Code 66177-15175, Sanandaj, Iran
[b] Research Centre for Medicinal Plant Breeding and Improvement, University of Kurdistan, Sanandaj, Iran

ARTICLE INFO

Article history:
Received 22 January 2013
Received in revised form 30 June 2013
Accepted 2 July 2013
Available online xxx

Keywords:
α-Hydroxyphosphonates
α-Acetoxyphosphonates
Magnetic nanoparticles Fe_3O_4
Guanidine
Basic catalyst

ABSTRACT

Magnetic nanoparticle Fe_3O_4-immobilized guanidine (MNPs-Guanidine) as a novel magnetically interphase nanocatalyst was synthesized and characterized. MNPs-Guanidine catalyzed the synthesis of α-hydroxyphosphonates from aldehydes and dimethyl phosphite in solvent-free condition at 80 °C. The synthesis of α-acetoxyphosphonates through a one-pot reaction of aldehydes, dimethyl phosphite and acetic anhydride was also achieved using this catalyst in PEG at room temperature. The catalyst was recycled up to 10 times with little loss of activity.

1. Introduction

The use of environmentally benign, sustainable, and efficiently reusable catalysts provides both economical and ecological benefits [1–3].

Magnetic separation from the reaction mixture is simple, economical, and promising for industrial applications [4–6]. This strategy is typically more effective than filtration or centrifugation [7]. Among the various magnetic nanoparticles as the core magnetic support, Fe_3O_4 nanoparticles are arguably the most extensively studied because of their intrinsic properties such as high surface area, low toxicity and superparamagnetic behavior [8,9,5,10–13]. In addition to that, all ferrites are metal oxides, presenting a large number of hydroxyl groups on the surface of their particles [14]. This characteristic allows building well-defined shells of different materials around the ferrite core or, when functional materials are targeted, grafting functional groups suitable for the supporting of all kinds of actuators, ligands and/or catalysts by covalent bonds [15].

The synthesis of α-hydroxyphosphonates and α-acetoxyphosphonateshas attracted much attention due to their potential biological activities with broad applications as synthetic intermediates [16–30].

Guanidines are important classes of compounds that have many uses within organic chemistry commonly as organic bases [31]. With the recent increase in interest in organocatalysis, they have also been shown to act as nucleophilic catalysts [32]. However the major disadvantage of catalysts based on guanidines is their separation from the products, which needs solid–liquid or liquid–liquid techniques in many reactions. This drawback can be overcome by immobilization these catalysts on magnetic nanoparticle (MNPs).

In continuation of our studies on environmentally benign chemical processes [33–35], in the present work we disclose that MNPs-Guanidine can be used as a novel magnetic interphase nanocatalyst for the synthesis of α-hydroxyphosphonates and α-acetoxyphosphonate.

2. Experimental

2.1. General remarks

The materials were purchased from Merck and Fluka and were used without any additional purification. All reactions were monitored by thin layer chromatography (TLC) on gel F254 plates. Melting points were obtained in open capillary tubes and also were

* Corresponding author at: Department of Chemistry, Faculty of Science, University of Kurdistan, Zip Code 66177-15175, Sanandaj, Iran. Tel.: +98 9183730910; fax: +98 8716624004.
E-mail addresses: a.rostami@uok.ac.ir, a_rostami372@yahoo.com, arostami372@gmail.com (A. Rostami).

0926-860X/$ – see front matter © 2013 Elsevier B.V. All rights reserved.
http://dx.doi.org/10.1016/j.apcata.2013.07.001

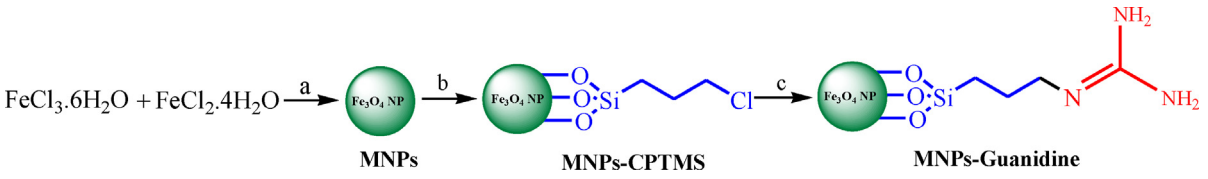

Scheme 1. (a) Aqueous ammonia, N_2, rt, 30 min; (b) (3-chloropropyl)-triethoxysilane, ethanol/water, 40 °C, 8 h; (c) guanidine hydrochloride, $NaHCO_3$, dry toluene, reflux, 28 h.

measured on an Electrothermal 9100 apparatus. The X-ray powder diffraction (XRD) data were collected on an X'Pert MPD. Philips diffractometer with Cu Ka radiation source (λ = 1.54050 Å) at 40 kV voltage and 40 mA current. The SEM image was obtained by VEGA TESCAN. The thermogravimetric analysis (TGA) was carried out on a Bähr STA 503 instrument (Germany) under air atmosphere, heating rate 10 °C/min. The magnetic measurements were carried out in a vibrating sample magnetometer (VSM, BHV-55, Riken, Japan) at room temperature.

2.2. Preparation of large-scale the magnetic Fe_3O_4 nanoparticles (MNPs)

$FeCl_3{\cdot}6H_2O$ (4.865 g, 0.018 mol) and $FeCl_2{\cdot}4H_2O$ (1.789 g, 0.0089 mol) were added to 100 mL deionized water and sonicated until the salts dissolved completely. Then, 10 mL of 25% aqueous ammonia was added quickly into the reaction mixture in one portion under N_2 atmosphere at room temperature followed by stirring about 30 min with mechanical stirrer. The black precipitate was washed with doubly distilled water (five times).

2.3. Preparation of MNPs coated by (3-chloropropyl)-trimethoxysilane (MNPs-CPTMS)

The obtained MNPs powder (1.5 g) was dispersed in 250 mL ethanol/water (volume ratio, 1:1) solution by sonication for 30 min, and then CPTMS (99%, 2.5 mL) was added to the mixture. After mechanical stirring under N_2 atmosphere at 33–38 °C for 8 h, the suspended substance was separated with centrifugation (RCF = 13,200 × *g* for 30 min). The settled product was re-dispersed in ethanol by sonication. The final sample was separated by an external magnet and washed five times with ethanol. The product stored in a refrigerator to use.

2.4. Preparation of guanidine-functionalized magnetic Fe_3O_4 nanoparticles (MNPs-Guanidine)

The MNPs-CPTMS (1 g) was dispersed in dry toluene (6–8 mL) by ultrasonication for 10 min. Subsequently, guanidine hydrochloride (0.382 g, 0.004 mmol) and sodium bicarbonate (0.672 g, 0.008 mmol) were added and the mixture was refluxed for 28 h. Then, the final product was separated by magnetic decantation and washed twice by dry CH_2Cl_2, EtOH and CH_2Cl_2 respectively to remove the unattached substrates. The product was stored in a refrigerator until use.

2.5. General procedure for the preparation of α-hydroxyphosphonate derivatives

MNPs-Guanidine (0.03 g) was added to a mixture of dimethyl phosphite (0.110 g, 1 mmol) and aldehyde (1 mmol) at 80 °C and stirred for 90–120 min. The progress was monitored by TLC. After completion of the reaction, the catalyst was separated by an external magnet and the mixture was washed with CH_2Cl_2 (2 × 5 mL) and decanted. The combined organics were dried over anhydrous Na_2SO_4 and then evaporation of dichloromethane under reduced pressure gave the pure products in 62–98% yields.

2.6. General procedure for the preparation of α-acetoxyphosphonate derivatives

MNPs-Guanidine (0.06 g) was added to a mixture of dimethyl phosphite (0.110 g, 1 mmol), aldehyde (1 mmol) and acetic anhydride (0.306 g, 3 mmol) in PEG (2 mL) at room temperature and stirred for the appropriate time. The progress was monitored by TLC. After completion of the reaction, the catalyst was separated by an external magnet and the mixture was washed with diethylether/water = 1:1 (3 × 20 mL). The combined organics were washed with brine (5 mL) and dried over anhydrous Na_2SO_4. The evaporation of diethylether under reduced pressure gave the pure products in 87–98% yields.

3. Results and discussions

3.1. Characterization of MNPs-Guanidine

The process of the preparation guanidine-functionalized magnetic Fe_3O_4 nanoparticles is shown in Scheme 1.

MNPs-Guanidine was characterized using a variety of different techniques. The XRD pattern of MNPs-Guanidine is shown in Fig. 1a. A weak broad band (2θ = 18–22°) appeared in MNPs-Guanidine pattern which could be assigned to the amorphous silane shell formed around the magnetic cores [36]. The lattice parameter was calculated for the prepared particles and compares these values with the standard parameters for magnetite.

The interlayer spacing (d_{hkl}), calculated using the Bragg equation, agrees well with the data for standard magnetite (Table 1).

Fig. 1b shows the SEM image of the synthesized guanidine loaded magnetite nanoparticles. It was confirmed that the catalyst was made up of uniform nanometer-sized particles less than 17 nm.

One indication of bond formation between the nanoparticles and the catalyst can be inferred from thermogravimetric analysis (TGA). TGA curve of the MNPs-Guanidine show the mass loss of the organic functional group as it decompose upon heating (Fig. 2a). The weight loss at temperatures below 200 °C is due to the removal of physically adsorbed solvent and surface hydroxyl groups [38,39]. Organic groups have been reported to desorb at temperatures above 260 °C. The curve shows a weight loss about 10% from 260 to 600 °C, resulting from the decomposition of organic spacer grafting to the MNPs surface.

EDX spectrum shows the elemental composition of the MNPs-Guanidine (Fig. 2b). Elemental analysis results showed that the

Table 1
Interlayer spacings (d_{hkl}) for MNPs-Guanidine.

Sample	d_{hkl} (Å)					
	1	2	3	4	5	6
Standard Fe_3O_4 [37]	2.96	2.53	2.09	1.71	1.61	1.48
MNPs-Guanidine	2.97	2.53	2.08	1.71	1.61	1.48

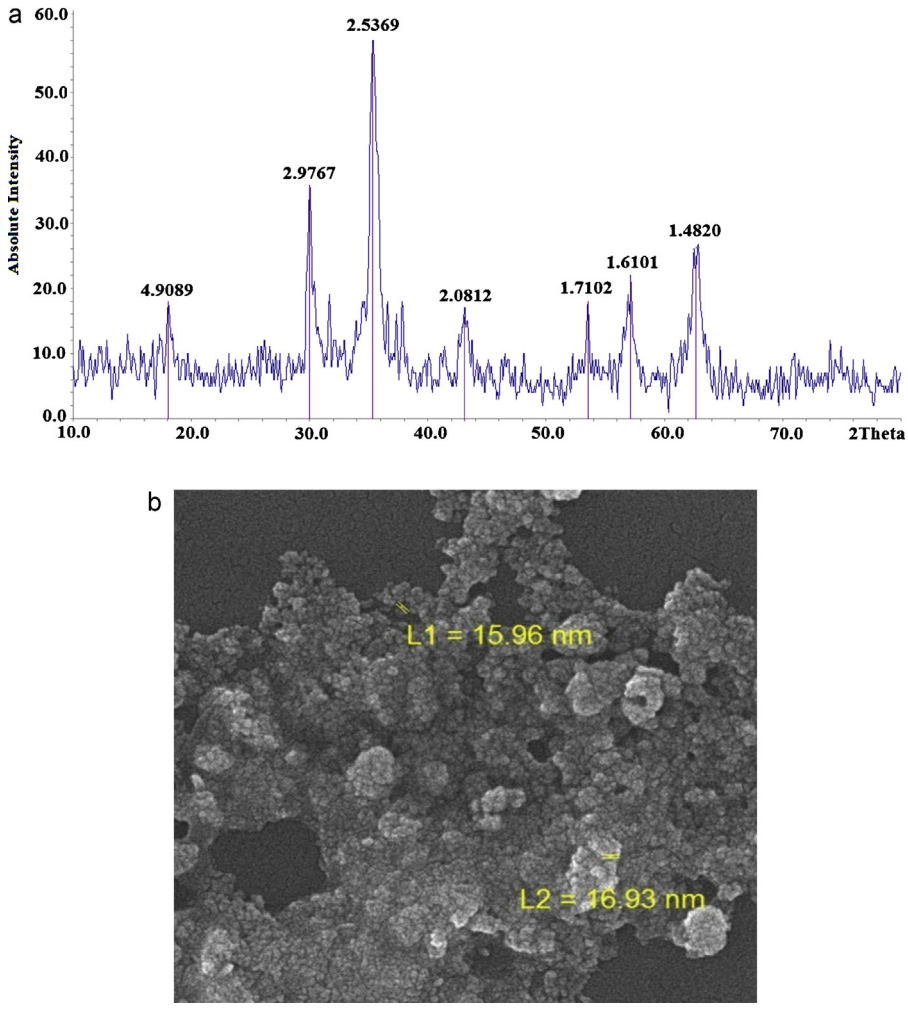

Fig. 1. (a) XRD pattern and (b) SEM image of the MNPs-Guanidine.

carbon, hydrogen, and nitrogen content of the MNPs-Guanidine was 5.7, 0.5, and 0.9 (wt%), respectively. The loading of the guanidine function on the magnetic nanoparticles was determined by elemental analysis of nitrogen as 0.22 mmol/g.

Fig. 3 shows Fourier transform infrared (FTIR) spectra for MNPs, MNPs-CPTMS, and MNPs-Guanidine. The FTIR spectrum for the MNPs alone shows a stretching vibration at 3418 cm^{-1} which incorporates the contributions from both symmetrical and asymmetrical modes of the O—H bonds which are attached to the surface iron atoms [9]. The bands at low wave numbers ($\leq$700 cm^{-1}) come from vibrations of Fe—O bonds of iron oxide, in which for the bulk Fe_3O_4 samples appear at 570 and 375 cm^{-1} but for Fe_3O_4 nanoparticles at 624 and 572 cm^{-1} as a blue shift, due to the size reduction [38,40,41]. The presence of an adsorbed water layer is confirmed by a stretch for the vibrational mode of water found at 1620 cm^{-1}. The FTIR spectra of MNPs-CPTMS and MNPs-Guanidine show Fe—O vibrations in the same vicinity. The introduction of CPTMS to the surface of MNPs is confirmed by the bands at 1005 and 1128 cm^{-1} assigned to the Fe—O—Si and C—Cl stretching vibrations respectively. Reaction of MNPs-CPTMS with guanidine produces MNPs-Guanidine in which the presence of guanidine moiety is asserted with 1443 and 3381 cm^{-1} bands corresponding to the C—N and N—H stretches respectively.

Superparamagnetic particles are beneficial for magnetic separation; the magnetic properties of MNPs and MNPs-Guanidine were characterized by a vibrating sample magnetometer (VSM). The room temperature magnetization curves of MNPs and MNPs-Guanidine is shown in Fig. 4a and b, respectively. As expected, the bare MNPs, showed the higher magnetic value (saturation magnetization, Ms) of 74.3 emu g^{-1} [42], the Ms value of MNPs-Guanidine is decreased due to the silica coating and the layer of the grafted catalyst (47.4 emu g^{-1}). It has been reported that the Fe_3O_4 nanoparticles with a value of coercivity (Hc) lower than 20 Oe could be called superparamagnetic. MNPs and MNPs-Guanidine have an Hc of 16.09 and 14.32 Oe, respectively and the remanent magnetization (Mr) of ~1.47 and 1.01 emu g^{-1}, respectively. As a result, the modified MNPs have a typical superparamagnetic behavior [43–45] and can be efficiently attracted with a small magnet.

Table 2
Optimization of the reaction conditions for the reaction of dimethyl phosphite (1 mmol) with benzaldehyde (1 mmol).

Entry	Solvent	Catalyst (mg)	Time (min)	Conversion (%)
1	Solvent-free, 80 °C	None	>1440	No reaction
2	Solvent-free, 80 °C	40	115	100
3	Solvent-free, 80 °C	30	120	100
4	Solvent-free, 80 °C	20	120	100
5	Solvent-free, 80 °C	15	120	100
6	Solvent-free, 80 °C	10	380	100
7	Solvent-free, rt	15	380	Trace
8	H_2O	15	380	Trace
9	PEG	15	380	No reaction
10	CH_3CN	15	380	No reaction

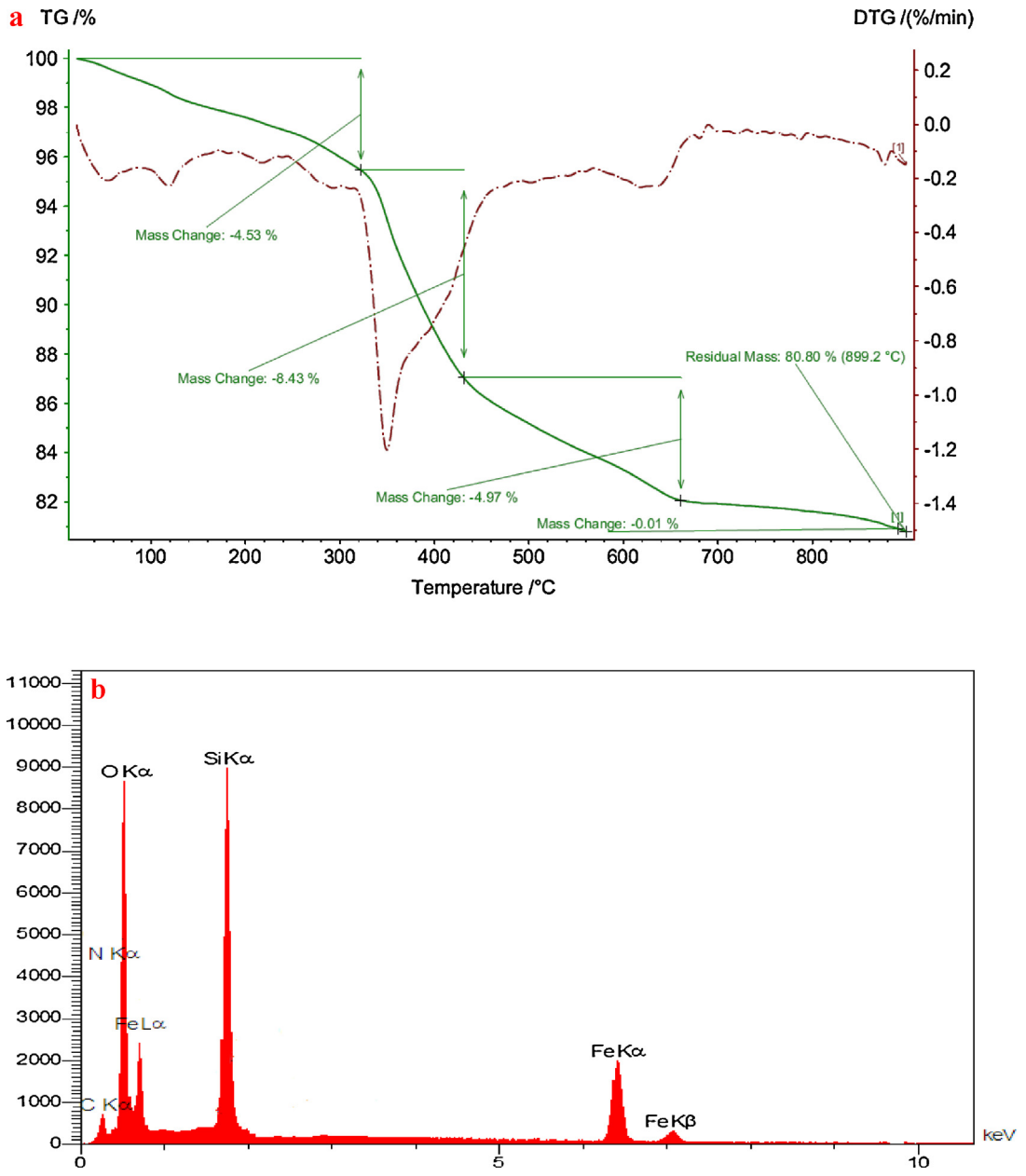

Fig. 2. (a) TGA profile and (b) EDX spectrum of the MNPs-Guanidine.

3.2. Application of MNPs-Guanidine for the synthesis of α-hydroxyphosphonates derivatives

MNPs-Guanidine was tested as basic magnetically separable heterogeneous nanocatalyst for the synthesis of the α-hydroxyphosphonates **(3a-p)** from reaction of wide range of aromatic aldehydes **1** with dimethyl phosphite **2** under solvent-free conditions at 80 °C (Scheme 2).

The investigation of the reaction conditions for the model hydrophosphonylation reaction between dimethyl phosphite (1 mmol) and benzaldehyde (1 mmol) in terms of the catalyst amount, reaction time and product yield demonstrated that 15 mg

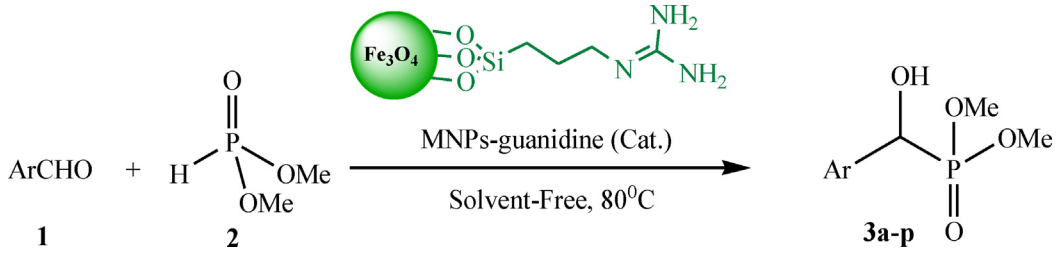

Scheme 2. MNPs-Guanidine catalyzes the preparation of α-hydroxyphosphonate derivatives.

Table 3
MNPs-Guanidine (15 mg) catalyzed the synthesis of α-hydroxyphosphonates from reaction of aldehydes (1 mmol) and dimethyl phosphite (1 mmol) in solvent-free conditions at 80 °C.

Entry	Aldehyde	Product	Time (min)	Yield (%)[a]
3a	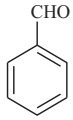	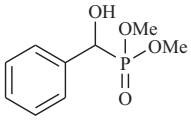	120	85
3b	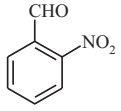	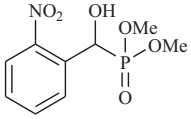	75	62
3c	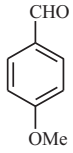	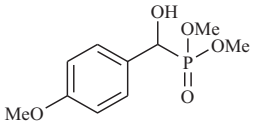	120	89
3d	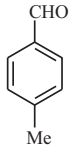	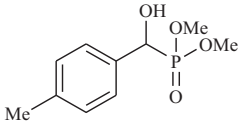	90	93
3e	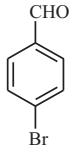	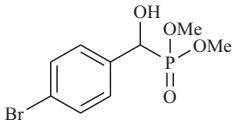	90	74
3f	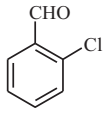	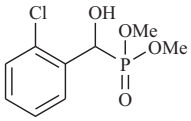	150	92
3g	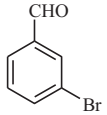	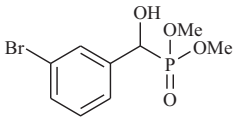	210	70
3h	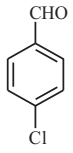	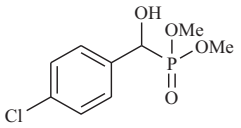	240	83
3i	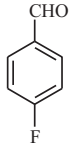	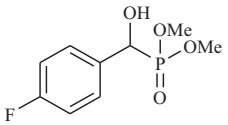	210	85
3j	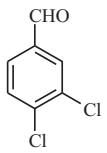	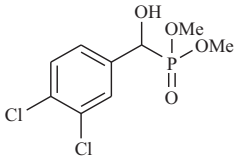	90	88

Table 3 (*Continued*)

Entry	Aldehyde	Product	Time (min)	Yield (%)[a]
3k	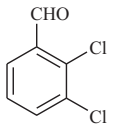	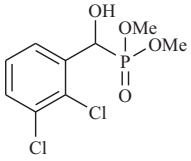	90	98
3l	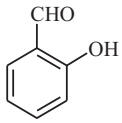	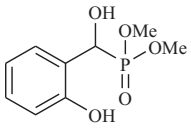	180	77
3m	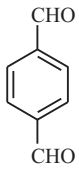	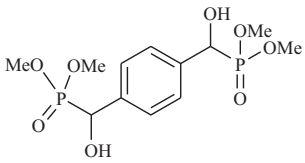	240	70
3n	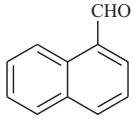	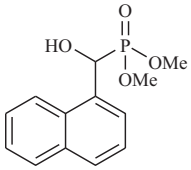	120	90
3o	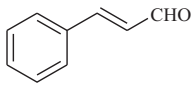	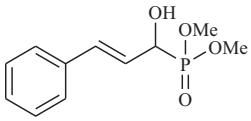	120	70
3p	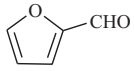	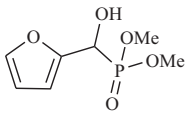	90	93

[a] All the products are known and were characterized by IR, ^{1}H NMR and ^{13}C NMR comparisons with those of authentic samples [24–27].

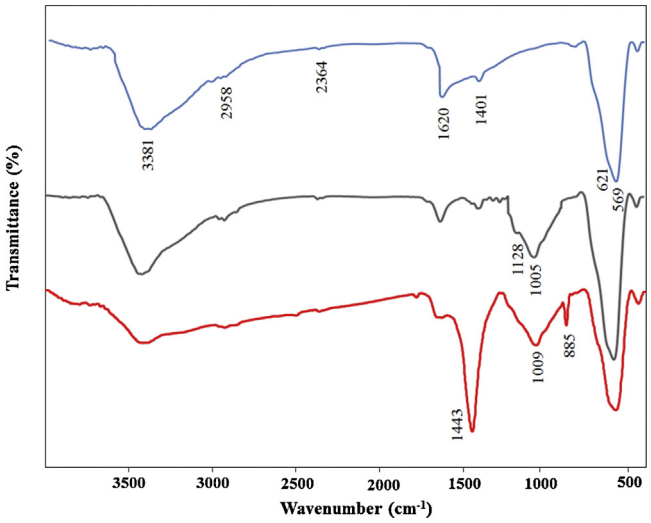

Fig. 3. FTIR spectra of MNPs (blue), MNPs-CPTMS (black) and MNPs-Guanidine (red). (For interpretation of the references to color in this figure caption, the reader is referred to the web version of the article.)

of the catalyst under solvent-free conditions at 80 °C was optimal for the desired reaction (Table 2, entry 5).

With the optimal conditions, the generality and the applicability of this method was further examined for the synthesis of α-hydroxyphosphonates from the reaction of dimethyl phosphite with structurally diverse aromatic aldehydes including different types of substituted benzaldehydes, cinnamaldehyde, 1-naphthaldehyde, and terephthaldehyde (Table 3). The results are summarized in (Table 3).

The feasibility of repeated use of MNPs-Guanidine was also investigated for the reaction of dimethyl phosphite with benzaldehyde. We found that this catalyst demonstrated excellent recyclability. The catalyst can be efficiently recovered easily and rapidly from the product by exposure to an external magnet (Fig. 5). To remove the residual product, the remaining magnetic nanoparticles were further washed with the EtOH, air-dried and used directly for the next round of reaction without further purification. The recycled catalyst was used for up to 10 runs with little loss of activity (Table 4).

In order to learn the efficiency and greenness of this method, we compared our obtained results for hydrophosphonylation of benzaldehyde with some data from the literature. We have found many of the previously reported methodologies suffer from one or more disadvantages such as using volatile and toxic organic solvents [24–29] and prolonged reaction times [26–29]. In addition,

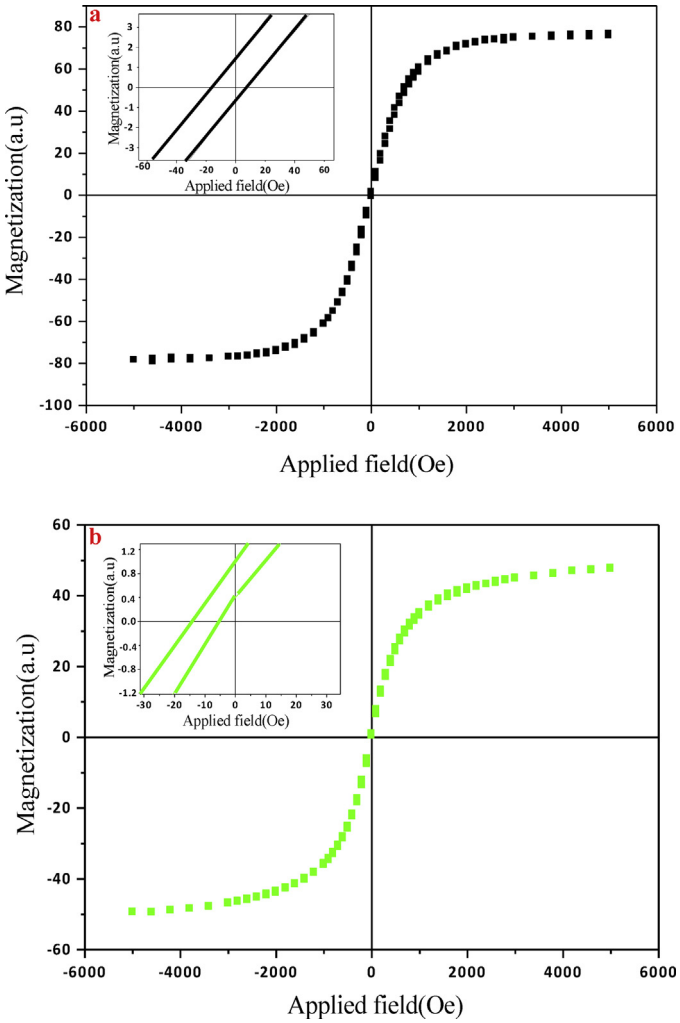

Fig. 4. (a) Hysteresis loop of the MNPs and (b) MNPs-Guanidine at room temperature (left inset: the magnified field from −30 to 30 Oe).

Table 4
Recycling of MNPs-Guanidine for the synthesis of 3a[a] and 5a.[b]

Cycle	Conversion (%) 3a	Conversion (%) 5a
1	100	100
2	100	100
3	100	100
4	100	100
5	100	97
6	96	95
7	96	95
8	90	90
9	85	83
10	80	78

[a] Reaction conditions: benzaldehydes (1 mmol), dimethyl phosphite (1 mmol), MNPs-Guanidine (15 mg), solvent-free, 80 °C, 120 min.
[b] Reaction conditions: benzaldehyde (1 mmol), dimethyl phosphite (1 mmol) acetic anhydride (3 mmol), MNPs-Guanidine (60 mg), PEG, rt 5 min.

the number of catalyst recycles is increased when the magnetic nanoparticles is used as alternative catalyst support. We believe the present method to be an improvement with respect to other procedures.

3.3. Application of MNPs-Guanidine in synthesis of α-acetoxyphosphonates derevatives

Owing to the success of MNPs-Guanidine for carrying out different reactions, we have studied the possibility of applying this new catalyst for the synthesis of α-acetoxyphosphonates in PEG at ambient temperature (Scheme 3).

To obtain the optimal reaction conditions, we evaluated the influence of solvent and different amounts of catalyst on the time and product yield in the reaction of benzaldehyde (1 mmol), dimethyl phosphite **2** (1 mmol) and acetic anhydride **4** (3 mmol), which was used as a model. In the absence of any catalyst, no reaction was observed even after prolonged reaction time. When the catalyst was added, the times were reduced. However 60 mg of MNPs-Guanidine in PEG was optimal for the desired reaction. Also, inferior results were obtained with H_2O, CH_3CN and under solvent-free conditions.

Fig. 5. Image showing MNPs-Guanidine can be separated by applied magnetic field. A reaction mixture in the absence (left) or presence of a magnetic field (right).

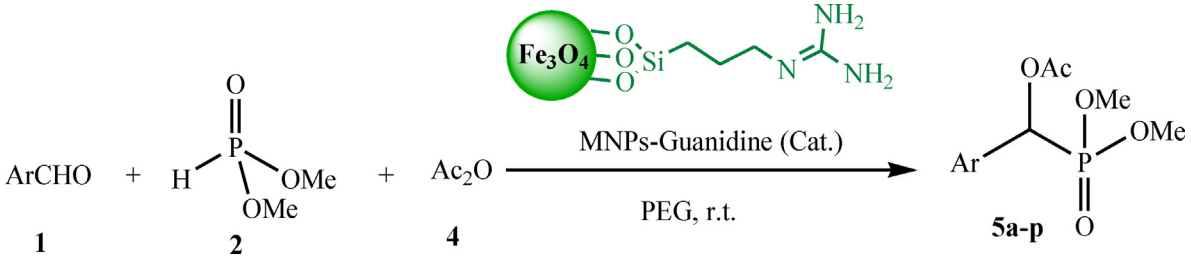

Scheme 3. MNPs-Guanidine catalyzes the synthesis of the α-acetoxyphosphonate derivatives.

Table 5
MNPs-Guanidine (60 mg) catalyzed the synthesis of α-acetoxyphosphonates from aldehyde (1 mmol), dimethyl phosphite (1 mmol) and acetic anhydride (3 mmol) in PEG at ambient temperature.

Entry	Aldehyde	Product	Time (min)	Yield (%)[a]
5a	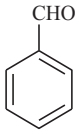	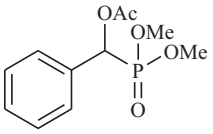	5	98
5b	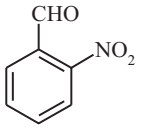	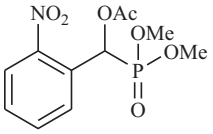	7	92
5c	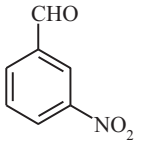	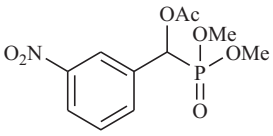	6	93
5d	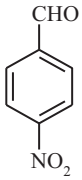	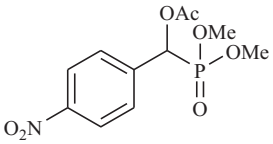	5	99
5e	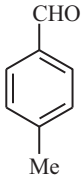	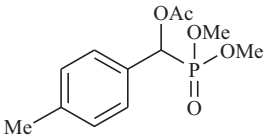	10	91
5f	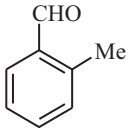	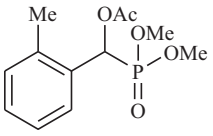	15	89
5g	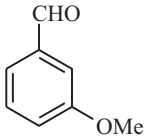	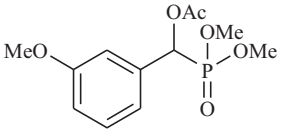	8	94
5h	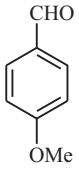	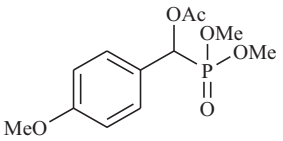	12	90
5i	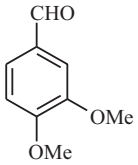	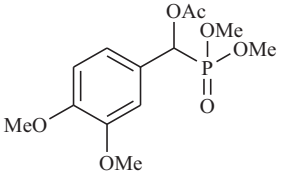	13	92
5k	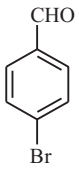	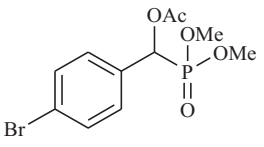	10	97

Table 5 (*Continued*)

Entry	Aldehyde	Product	Time (min)	Yield (%)[a]
5l	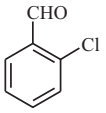	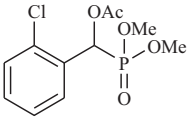	15	96
5m	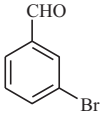	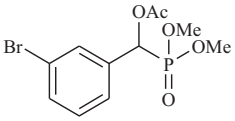	6	89
5n	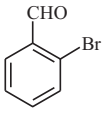	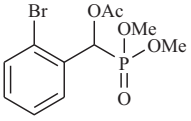	8	95
5o	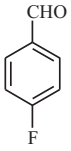	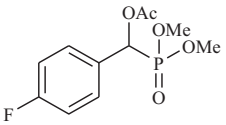	5	94
5p	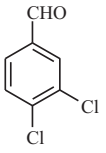	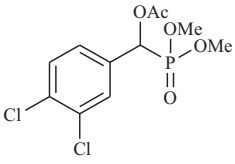	6	95

[a] All the products are known and were characterized by IR, ^{1}H NMR and ^{13}C NMR with those of authentic samples [30].

Subsequently, a series of differently α-acetoxyphosphonates derivatives were prepared successfully under optimal conditions. These results are listed in Table 5. In all cases, up to quantitative yields in reasonable reaction times were obtained.

We also investigated the recycling of the catalyst using model reaction of benzaldehyde (1 mmol) with dimethyl phosphite (1 mmol) and acetic anhydride (3 mmol). The recovered catalyst was reused for at least 10 runs with little loss of activity (Table 4).

4. Conclusion

In summary, we have synthesized the first MNPs-Guanidine for use as a magnetically heterogeneous basic nanocatalyst. The catalyst is easily synthesized and can catalyze the synthesis of α-hydroxyphosphonates and α-acetoxyphosphonates with good to high yields in different conditions. The characteristic aspects of this catalyst are rapid, simple and efficient separation by using an appropriate external magnet, which minimizes the loss of catalyst during separation and reusable for several times with little loss of activity. In addition, MNPs-Guanidine couples the advantages of heterogeneous and homogeneous guanidine-based systems, which make it a promising material for industrial.

Acknowledgment

We are grateful to the University of Kurdistan Research Councils for partial support of this work.

References

[1] B.M. Trost, Science 245 (1991) 1471–1477.
[2] P.T. Anastas, J.C. Warner, Green Chem. Theory and Practice, Oxford University Press, Oxford, 1998.
[3] J.F. Jenck, F. Agterberg, M.J. Droescher, Green Chem. 6 (2004) 544–556.
[4] S. Sun, H. Zeng, J. Am. Chem. Soc. 124 (2002) 8204–8205.
[5] A.H. Latham, M.E. Williams, Acc. Chem. Res. 41 (2008) 411–420.
[6] S. Laurent, D. Forge, M. Port, A. Roch, C. Robic, L. Vander Elst, R.N. Muller, Chem. Rev. 108 (2008) 2064–2110.
[7] D. Guin, B. Baruwati, S.V. Manorama, Org. Lett. 9 (2007) 1419–2142.
[8] C.Ó. Dálaigh, S.A. Corr, Y. Gunko, S.J. Connon, Angew. Chem. Int. Ed. 46 (2007) 4329–4332.
[9] S. Luo, X. Zheng, H. Xu, X. Mi, L. Zhang, J.-P. Cheng, Adv. Synth. Catal. 349 (2007) 2431–2434.
[10] S. Shylesh, V. Schunemann, W.R. Thiel, Angew. Chem. Int. Ed. 49 (2010) 3428–3452.
[11] C. Boyer, M.R. Whittaker, V. Bulmus, J. Liu, T.P. Davis, NPG Asia Mater. 2 (2010) 23–30.
[12] Y. Zhu, L.P. Stubbs, F. Ho, R. Liu, C.P. Ship, J.A. Maguire, N.S. Hosmane, Chem. Cat. Chem. 2 (2010) 365–374.
[13] C.W. Lim, I.S. Lee, Nano Today 5 (2010) 412–434.
[14] E. McCafferty, J.P. Wightman, Surf. Interface Anal. 26 (1998) 549–564.
[15] P. Riente, C. Mendozaa, M.A. Peric, J. Mater. Chem. 21 (2011) 7350–7355.
[16] B. Kaboudin, Tetrahedron Lett. 44 (2003) 1051–1053.
[17] B. Kaboudin, F. Saadati, Synthesis (2004) 1249–1252.
[18] R.U. Pokalwar, R.V. Hangarge, P.V. Maske, M.S. Shingare, Arkivoc 6 (2006) 196–204.
[19] D.Q. Shi, Z.L. Sheng, X.P. Liu, H. Wu, Heteroat. Chem. 14 (2003) 266–268.
[20] A.J. Ganzhorn, J. Hoflack, P.D. Pelton, F. Strasser, M.C. Chanal, S.R. Piettre, Bioorg. Med. Chem. 6 (1998) 1865–1874.
[21] A. Szymanska, M. Szymczak, J. Boryski, J. Stawinski, A. Kraszewski, G. Collu, G. Sanna, G. Giliberti, R. Loddo, P.L. Colla, Bioorg. Med. Chem. 14 (2006) 1924–1934.
[22] M. Drescher, F. Hammerschmidt, H. Kahlig, Synthesis (1995) 1267–1272.
[23] G. Eidenhammer, F. Hammerschmidt, Synthesis (1996) 748–754.
[24] Q. Wu, J. Zhou, Z. Yao, F. Xu, Q. Shen, J. Org. Chem. 75 (2010) 7498–7501.
[25] M. Pandi, P.K. Chanani, S. Govindasamy, Appl. Catal. A: Gen. 441 (2012) 119–123.
[26] R.G. Noronha, P.J. Costa, C.C. Romao, M.J. Calhorda, A.C. Fernandes, Organometallics 28 (2009) 6206–6212.
[27] S. Gou, X. Zhou, J. Wang, X. Liu, X. Feng, Tetrahedron 64 (2008) 2864–2870.
[28] W. Chen, Y. Hui, X. Zhou, J. Jiang, Y. Cai, X. Liu, L. Lin, X. Feng, Tetrahedron Lett. 51 (2010) 4175–4178.
[29] K. Suyama, Y. Sakai, K. Matsumoto, B. Saito, T. Katsuki, Angew. Chem. Int. Ed. 49 (2010) 797–799.
[30] B. Kaboudin, M. Karimi, Arkivoc xiii (2007) 124–132.
[31] T. Ishikawa, Superbases for Organic Synthesis: Guanidines, Amidines, Phosphazenes and Related Organocatalysts, Wiley, Chippenham, 2009.
[32] J.E. Taylor, S.D. Bull, J.M.J. Williams, Chem. Soc. Rev. 41 (2012) 2109–2121.
[33] A. Rostami, J. Akradi, Tetrahedron Lett. 51 (2010) 3501–3503.

[34] A. Rostami, A. Yari, J. Iran. Chem. Soc. 9 (2012) 489–493.
[35] H. Jafari, A. Rostami, F. Ahmad-Jangi, A. Ghorbani-Choghamarani, Synth. Commun. 42 (2012) 3150–3156.
[36] Y. Jiang, J. Jiang, Q. Gao, M. Ruan, H. Yu, L. Qi, Nanotechnology 19 (2008) 75714–75719.
[37] F. Brackmann, H. Schill, A. Meijere, Chem. Eur. J. 11 (2005) 6593–6600.
[38] M.Z. Kassaee, H. Masrouri, F. Movahed, Appl. Catal. A: Gen. 395 (2011) 28–33.
[39] R.M. Cornell, U. Schwertmann, The Iron Oxides, VCH, New York, 1996.
[40] Z.M. Rao, T.H. Wu, S.Y. Peng, Acta Phys. Chim. Sin. 11 (1995) 395–399.
[41] R.D. Waldron, Phys. Rev. 99 (1955) 1727–1735.
[42] K. Naka, A. Narital, H. Tanakal, Y. Chujo, M. Morita, T. Inubushi, I. Nishimura, J. Hiruta, H. Shibayama, M. Koga, S. Ishibashi, J. Seki, S. Kizaka-Kondoh, M. Hiraoka, Polym. Adv. Technol. 19 (2008) 1421–1429.
[43] R.C. Ohandley, Modern Magnetic Materials: Principles and Applications, Wiley, New York, 2000.
[44] R.H. Iida, K. Takayanagi, T. Nakanishi, T.J. Osaka, Colloid Interface Sci. 314 (2007) 274–280.
[45] G.W. Cheng-Lin, H. Huan, G. Hong-Jun, L. Gan, M. Ru-Jiang, A. Ying-Li, S. Lin-Qi, Sci. China Chem. 53 (2010) 514–518.